Title
Mechanistic Insights into Two-Phase Radical C-H Arylations.

Journal
ACS central science, 1(8)

ISSN
2374-7943

Authors
Baxter, Ryan D
Liang, Yong
Hong, Xin
et al.

Publication Date
2015-11-01

DOI
10.1021/acscentsci.5b00332

Peer reviewed

ACS central science

Research Article

http://pubs.acs.org/journal/acscii

Mechanistic Insights into Two-Phase Radical C–H Arylations

Ryan D. Baxter,[†] Yong Liang,[‡] Xin Hong,[‡] Timothy A. Brown,[§] Richard N. Zare,*[,§] K. N. Houk,*[,‡] Phil S. Baran,*[,†] and Donna G. Blackmond*[,†]

[†]Department of Chemistry, The Scripps Research Institute, La Jolla, California 92037, United States

[‡]Department of Chemistry and Biochemistry, University of California, Los Angeles, California 90095, United States

[§]Department of Chemistry, Stanford University, Stanford, California 94305, United States

Supporting Information

ABSTRACT: Kinetic, spectroscopic, and computational studies of radical C–H arylations highlight the interplay between chemical and physical rate processes in these multiphase reactions. Anomalous concentration dependences observed here may be reconciled by considering the role of phase transfer processes that mediate concentrations in each phase. In addition, understanding interactions through phase boundaries enables their use in optimization of reaction performance.

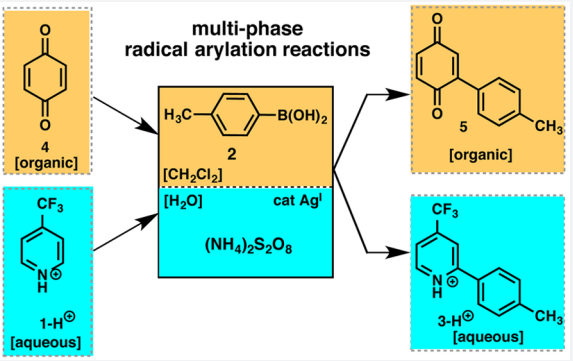

Mechanistic studies of multistep organic reactions focus on understanding the concentration driving forces and the nature of key intermediate species in the sequence of elementary reaction steps comprising the overall transformation. In cases where the reaction medium is multiphase, however, interpretation of experimental observations may be complicated by the convolution of intrinsic chemical kinetics with mass transfer rate processes. A prominent example is found in asymmetric catalytic hydrogenation, where gas–liquid mass transfer control of the global rate may strongly influence product enantioselectivity.[1] The presence of two immiscible liquid phases may also influence reactions, with Schotten–Baumann reaction conditions representing a classic case where system properties are exploited to optimize the reaction.[2] Reports of rate acceleration for organic reactions in water include Breslow's classic studies of hydrophobic effects in Diels–Alder reactions[3] and Sharpless's "on water" effect for water-insoluble organics.[4] The concept of employing immiscible phases to alter reaction outcomes is being extended to areas as far-reaching as controlling nanoparticle synthesis in microfluidic segmented flow[5] and the development of protocells in studies probing the origin of life.[6] Most recently, an innovative approach used phase behavior to carry out oxidation and reduction in a single vessel.[7]

Empirical optimization of multiphase reaction conditions in reactions of pharmaceutical interest highlights both the potential problems and notable advantages derived from multiphase systems. The recently reported direct metal-catalyzed C–H functionalization of heterocycles[8a] and quinones[8b] using arylboronic acids, conceived as a mechanistic parallel to Minisci free radical chemistry,[9] contains as many as six different components present in three different phases: solid or aqueous phase oxidant, organic or aqueous phase substrates, organic or aqueous phase catalyst, organic phase products. These single-electron oxidation reactions exhibit broad substrate scope, operational simplicity, and low catalyst cost[8] under mild conditions without prefunctionalization of the substrate and without direct addition to an arylmetalate;[8] however, a number of mechanistic questions, perhaps related to phase transfer considerations, remain unanswered.[10]

We report here detailed kinetic, spectroscopic, and computational investigations of the two-phase radical arylation reactions of pyridine **1** residing in protonated form in the aqueous phase and benzoquinone **4** found in the organic phase, as depicted in Scheme 1. The reactions employ $AgNO_3$ as catalyst and $(NH_4)_2S_2O_8$ as oxidant, both of which reside in the aqueous phase, and arylation partner *p*-tolylboronic acid **2** found in the organic phase. These studies are aimed not only at developing a mechanistic understanding of the intrinsic chemical reaction steps but also at probing the influence of phase transfer processes and their potential as a tool for reaction optimization.

Kinetic profiles are shown in Figures 1–3 for arylations of 4-CF_3-pyridine **1** and benzoquinone **4** as a function of substrate, oxidant, and catalyst concentrations. The reactions exhibit zero-order dependence on the concentration of *p*-tolylboronic acid **2** (Figure 1) and positive-order dependence on both $[(NH_4)_2S_2O_8]$ (Figure 2) and $[AgNO_3]$ (Figure 3). Comparison of the shapes of the kinetic profiles for the reactions of **1** and **4** in Figure 1, as well as the kinetic plots of reactions

Received: October 5, 2015
Published: November 2, 2015

DOI: 10.1021/acscentsci.5b00332
ACS Cent. Sci. 2015, 1, 456–462

Scheme 1. Arylation Reactions in Multiphase Systems

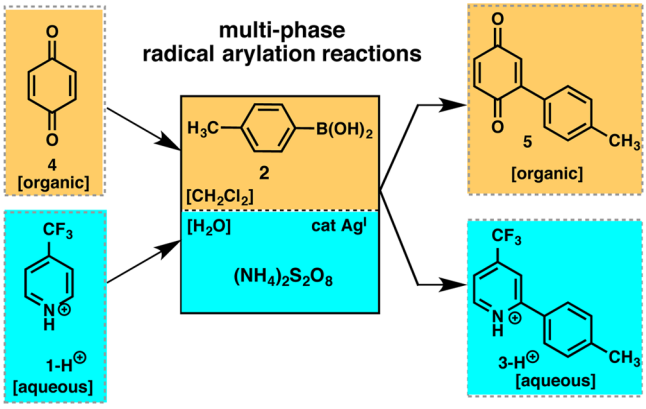

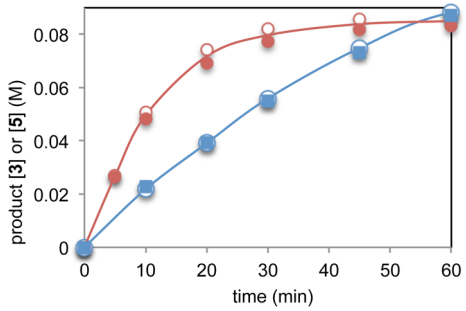

Figure 1. Effect of concentration of *p*-tolylboronic acid **2** on the temporal product concentration in the reactions of Scheme 1. Red symbols: CF_3-pyridine **1** (0.1 M) to form product **3**. Blue symbols: benzoquinone **4** (0.1 M) to form product **5**. Solid symbols: 0.15 M *p*-tolylboronic acid **2**. Open symbols: 0.3 M *p*-tolylboronic acid **2**. 20 mol % $Ag(NO_3)$ as catalyst, 0.3 M $(NH_4)_2S_2O_8$; CH_2Cl_2:H_2O = 1:1; T = 25 °C. Reactions with **1** include 1 equiv of TFA (see Supporting Information).

varying initial concentrations in Figure 3, reveals that the arylation exhibits positive-order kinetics in [**1**] and close to zero-order kinetics in [**4**]. Understanding these observations requires consideration not only of the intrinsic reactivity of each substrate but also of the mass transfer processes occurring in each case.

The reaction sequence is initiated by interaction between the catalyst and persulfate to produce sulfate radical anions ($SO_4^{-\bullet}$). The catalyst and the oxidant both reside in the aqueous phase, and the rate of $SO_4^{-\bullet}$ formation represents an intrinsic kinetic driving force that depends on both persulfate and catalyst concentrations, as is confirmed by the positive rate dependence on both concentrations. Free radicals react in the phase in which they are formed, being too short-lived to undergo productive reaction after mass transfer across a phase boundary. However, in order for the reaction to proceed, sulfate radical anions formed in the aqueous phase must interact with arylboronic acid **2**, which resides in the organic phase.

Figure 1 shows that zero-order kinetics in the arylboronic acid **2** is observed under all conditions, contrary to a previous study reporting a negative order in the concentration of [**2**] in the reaction of **1**.[11,12] Zero-order dependences are often attributed to chemical kinetic phenomena, for example saturation kinetics in catalytic reactions, or introduction of a substrate to an intermediate after the rate-determining step in the reaction, as for nucleophile concentration in S_N1 reactions.

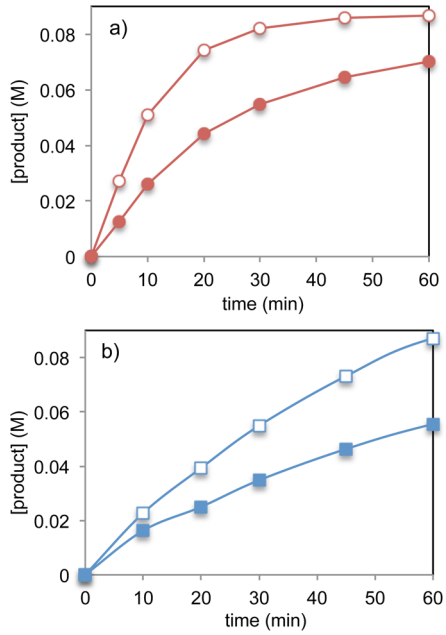

Figure 2. Effect of $(NH_4)_2S_2O_8$ oxidant concentration on temporal product concentration for the reactions of Scheme 1. Top: CF_3-pyridine **1** (0.1 M). Bottom: benzoquinone **4** (0.1 M). Solid symbols: 0.15 M $(NH_4)_2S_2O_8$. Open symbols: 0.3 M $(NH_4)_2S_2O_8$. 20 mol % $Ag(NO_3)$ as catalyst, 0.15 M *p*-tolylboronic acid **2**; CH_2Cl_2:H_2O = 1:1; T = 25 °C. Reactions with **1** include 1 equiv of TFA (see Supporting Information).

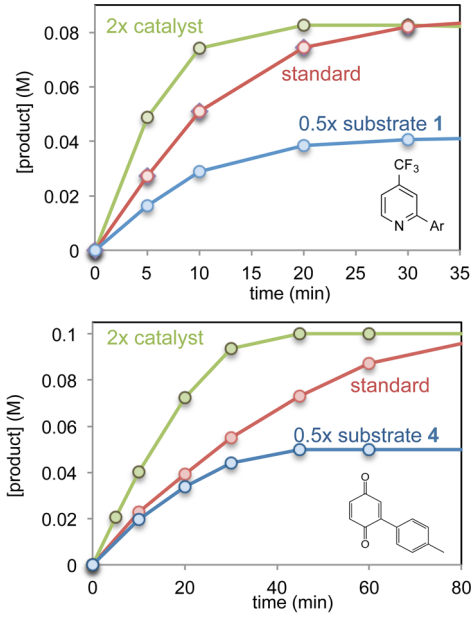

Figure 3. Kinetics of formation of products **3** (top) and **5** (bottom) as a function of initial concentrations of substrates **1** and **4** and of catalyst $AgNO_3$. Standard (red): $[\mathbf{1}]_0$, $[\mathbf{4}]_0$ = 0.1 M; $[\mathbf{2}]_0$ = 0.3 M; $[AgNO_3]$ = 0.02 M. 2× catalyst (green): $[AgNO_3]$ = 0.04 M. 0.5× substrate (blue): $[\mathbf{1}]_0$, $[\mathbf{4}]_0$ = 0.05 M. CH_2Cl_2:H_2O = 1:1; T = 25 °C. 1 equiv of TFA added in reactions of **1**.

However, control of the observed rate due to a mass transfer process may also result in observed zero-order kinetics if the concentration of a reacting species is mediated by a phase boundary. In general, zero-order kinetics due to mass transfer considerations may be attributed either to reaction steps in

DOI: 10.1021/acscentsci.5b00332
ACS Cent. Sci. 2015, 1, 456−462

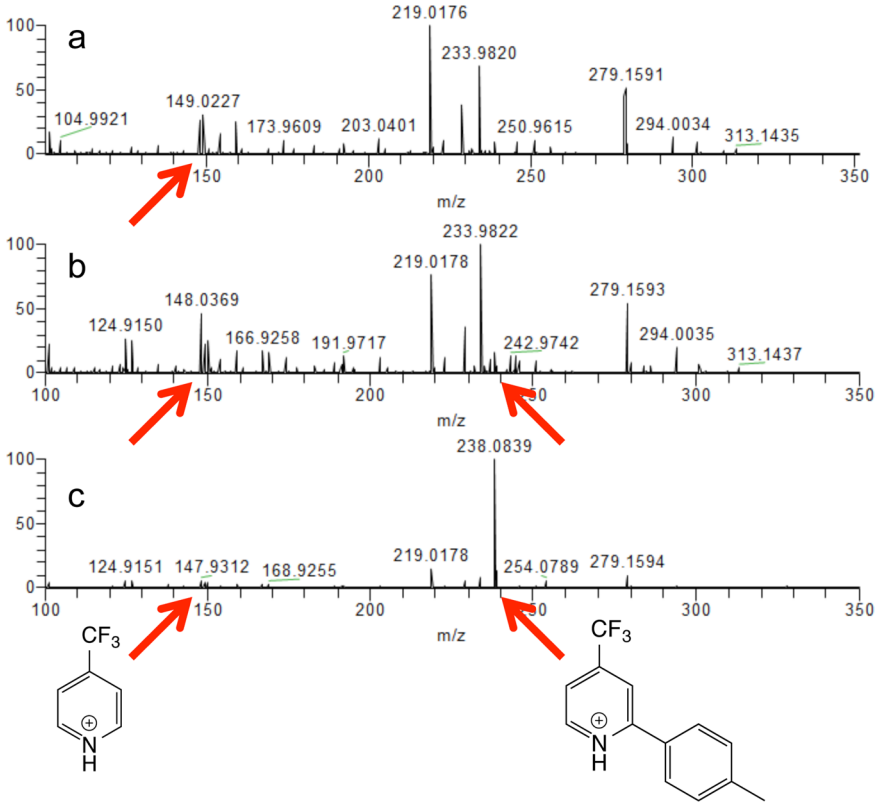

Figure 4. Mass spectroscopic monitoring of the $AgNO_3$-catalyzed reaction between **1** and **2** in the aqueous phase: (a) aqueous phase prior to addition of catalyst; (b) aqueous phase immediately after addition of catalyst; (c) aqueous phase after 10 min reaction time. Protonated substrate: *m*/*z* 148.0369 (100.0%), 149.0402 (6.5%); Protonated product: *m*/*z* 238.0838 (100.0%); 239.0872 (14.1%).

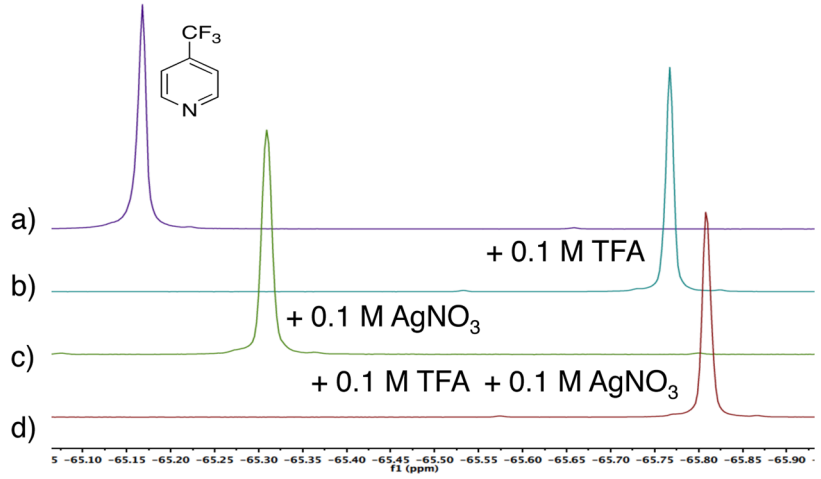

Figure 5. ^{19}F-NMR studies of the interaction between $AgNO_3$ and **1** in D_2O in the presence and absence of added acid: (a) 0.1 M **1**; (b) 0.1 M **1** with 0.1 M trifluoroacetic acid (TFA); (c) 0.1 M **1** with 0.1 M $AgNO_3$; (d) 0.1 M **1** with 0.1 M $AgNO_3$ and 0.1 M TFA.

which components meet across phase boundaries or to reactions where the concentration of a substrate is controlled by its mass transfer across a phase boundary. In the first scenario, aryl radical formation would take place at the aqueous/organic phase boundary when the sulfate radical anion and arylboronic acid meet, the mechanistic details of which might be similar to the related Minisci decarboxylation reaction. In the second case, while the arylboronic acid resides mainly in the organic phase, a small concentration may partition into the aqueous phase where boronic acid **2** would continually be replenished by mass transfer across the aqueous−organic phase boundary even as it is consumed in formation of aryl radicals $Ar^{\bullet}$. The resulting constant low concentration of **2** in the aqueous phase causes the reaction rate to appear as zero-order in [**2**].

Further evidence for the partitioning of **2** into the aqueous phase is found from electrospray ionization mass spectrometry (ESI-MS) experiments shown in Figure 4. This technique has been shown to be an effective tool in elucidating reaction pathways.[13−17] Protonated pyridine **1** is observed in the aqueous phase prior to addition of $AgNO_3$ catalyst (Figure 4a); surprisingly, reaction product **3** appears immediately upon

DOI: 10.1021/acscentsci.5b00332
ACS Cent. Sci. 2015, 1, 456−462

addition of the catalyst to the aqueous phase, implying partitioning of the arylboronic acid into the aqueous phase (Figure 4b). Arylated product **3** is the main species in the spectrum after 10 min reaction time. This result supports the kinetic results suggesting that the reaction of Ar• proceeds in the aqueous phase where it was formed.

A previous study by Flowers and co-workers[11] proposed that reactions of **1** proceed via a silver−pyridine complex that serves as the active catalyst. Importantly, no evidence was found in these mass spectroscopic experiments for this Ag-bound substrate. A small peak attributed to the Ag-bound product was observed, but in extremely low concentration, less than 0.5% of the total Ag catalyst employed.

^{19}F-NMR studies (Figure 5) showed that addition of $AgNO_3$ to pyridine **1** caused a small shift in the main peak at −65.15 ppm to −65.3 ppm, as had been reported,[11] but this shift is less than that caused by addition of acid to **1** in the absence of $AgNO_3$ (to −65.75 ppm). Addition of $AgNO_3$ to **1** in the presence of acid caused this peak to shift by an even smaller amount to −65.8 ppm. Mixing a stoichiometric amount of **1** with $AgNO_3$ in D_2O led to precipitation of a species that may indicate formation of a silver−pyridine complex denoted [**1**·Ag].

The efficacy of this [**1**·Ag] precipitate used as a catalyst was tested in the reaction of substrate **4**. Figure 6 shows that the

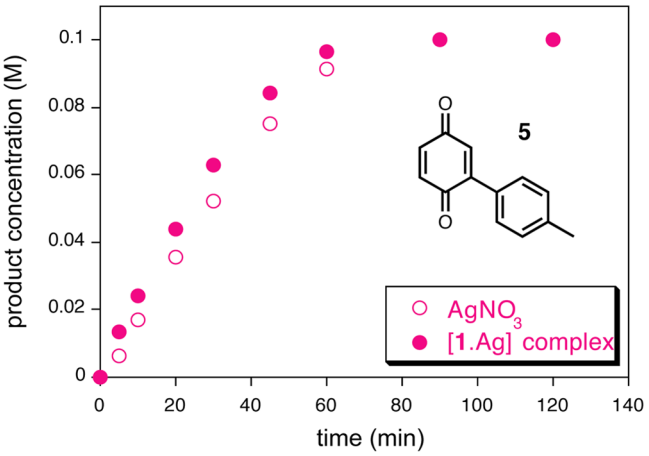

Figure 6. Kinetic profiles for reaction of **4** with **2** using $AgNO_3$ (open circles) or the complex [**1**·Ag] (filled circles) as catalyst; $[\mathbf{4}]_0$ = 0.1 M; $[\mathbf{2}]_0$ = 0.15 M; 20 mol % catalyst; CH_2Cl_2:H_2O = 1:1.

activity of the precipitated material is similar to that of $AgNO_3$ in the reaction of **4** in the absence of **1**. Further, adding the precipitate to water at the concentration employed in reactions showed that it dissolved back to free **1**, suggesting that **1** is not required to form the active Ag catalyst. Invoking a role for a [**1**·Ag] complex appears to be unnecessary to rationalize the results for reactions of **1** or **4** and $AgNO_3$ as catalyst in these arylations with arylboronic acid **2**.

Figure 3 also revealed that the reaction of **1** appears to follow first order kinetics in [**1**] while for **4** the rate is nearly insensitive to [**4**]. Such obervations might suggest that substrate **1** participates in the rate-limiting step while substrate **4** is not involved in the rate-determining step. Again, mass transfer processes across the phase boundary may rationalize this difference between the two reactions. Reaction between Ar• and substrate occurs in the aqueous phase where the free radical is formed. In the case of **1**, the intrinsic kinetic dependence is observed because **1** resides in the aqueous phase. For substrate **4**, however, mass transfer across the aqueous/organic interface must occur in order for the reaction to proceed. If the partitioning of **4** into the aqueous phase is small, the global rate may be insensitive to the overall concentration of **4**. In such a case the global kinetics may not be reflective of the intrinsic kinetic rate-determining step.

These studies demonstrate the importance of mass transfer processes in mediating the delivery of active species in reaction steps for reactions occurring under two-phase conditions. Further studies were carried out to probe the intrinsic chemical steps in the reaction network, most importantly kinetic isotope effects and computational modeling. A recent essay by Simmons and Hartwig[18] discussed comparison of the results of KIE experiments taken from separate rate measurements that differ from those obtained from competitive reactions carried out in a single flask in the context of distinguishing between potential rate-determining elementary reaction steps in multistep reactions. However, in multiphase systems such as those under study here, the convolution of chemical mass transfer rate processes must be also considered.[19] The study of kinetic isotope effects carried out in competitive vs parallel reactions may help to probe these complexities in multiphase systems.

H/D kinetic isotope effects were probed by comparing reaction kinetics for normal and deuterated substrates **1**-D and **4**-D. Figure 7 shows that neither reaction exhibited a

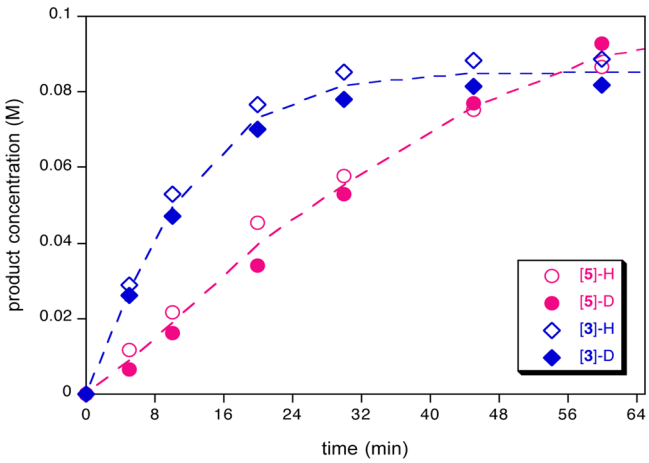

Figure 7. Kinetics of formation of product **3** and **5** from reactions using **1**-H and **1**-D and **4**-H and **4**-D. $[\mathbf{1}]_0$, $[\mathbf{4}]_0$ = 0.1 M; $[\mathbf{2}]_0$ = 0.15 M; 20 mol % catalyst; CH_2Cl_2:H_2O = 1:1; 1 equiv of TFA added to reactions of **1**.

discernible KIE in global kinetic experiments. Competition KIE experiments, in which normal and deuterated substrate are present in the same flask and relative rather than absolute rates are measured, corroborated the lack of a substantial KIE (k_H/k_D = 0.96 for **4** and k_H/k_D = 1.04 for **1**).

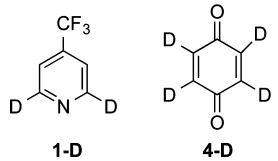

1-D **4-D**

Kinetic isotope effects of important reaction steps were calculated for the addition of Ar• to each substrate (protonated pyridine **1** and benzoquinone **4**) and the subsequent

DOI: 10.1021/acscentsci.5b00332
ACS Cent. Sci. 2015, 1, 456−462

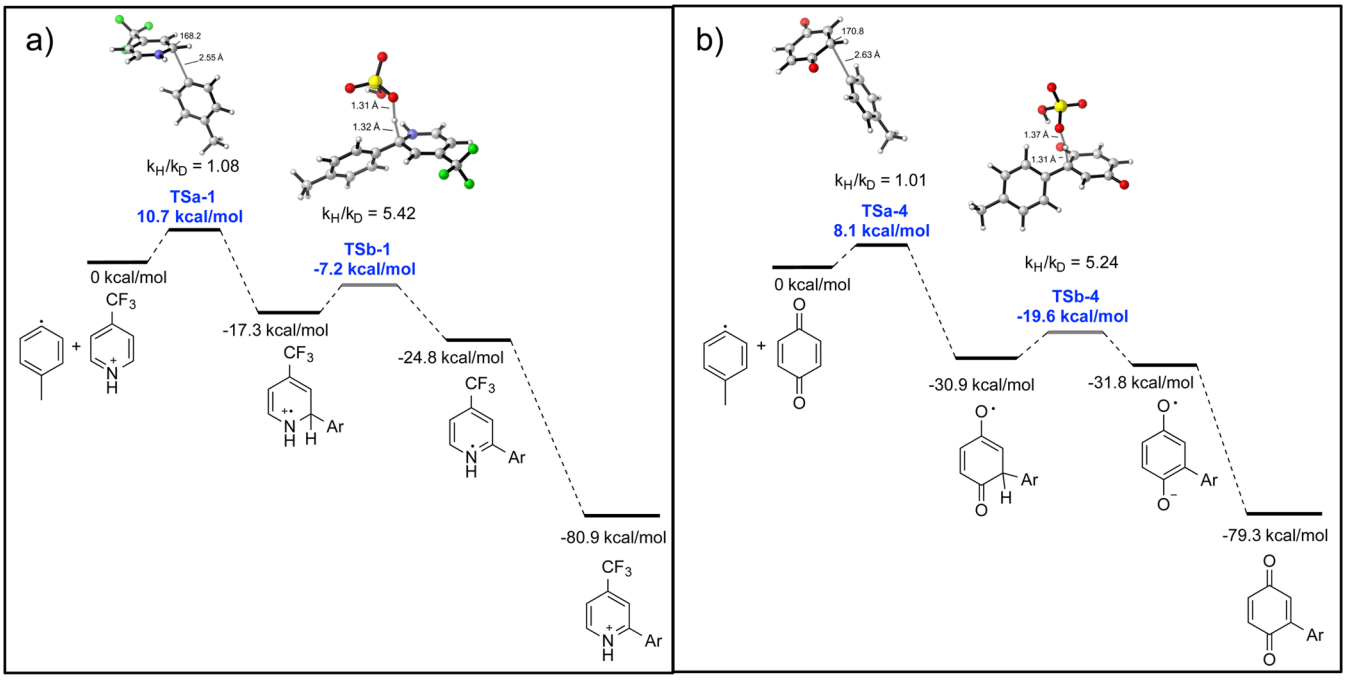

Figure 8. Energy diagram and computed KIE values for aryl radical addition and C−H abstraction steps.

abstraction of a proton. Free energy surfaces and KIEs were computed at the CPCM(water)-M06-2*X*/6-311+G(d,p)//B3LYP/6-31+G(d) level of theory. The computational results shown in Figure 8 indicate that addition of the aryl radical to the substrate should give similar rates for H and D substrates, while abstraction of the proton should yield a strong normal KIE. Both the strong exothermicity of $Ar^{\bullet}$ addition and the lack of an observed KIE under competitive conditions suggest that aryl radical addition to the substrate is irreversible and rate-determining. However, this conclusion predicts positive-order kinetics in substrate concentration, which is supported by the experimental observations for the reaction of **1** but is at odds with the observed zero-order kinetics in [**4**]. As was suggested earlier, invoking a contribution from a mass transfer process could provide a resolution to this contradiction. Diffusion through the phase boundary provides a low, steady-state concentration of **4** to react with $Ar^{\bullet}$ in the aqueous phase, resulting in the observation of pseudo-zero-order kinetics even while **4** is involved in the rate-determining step.

The calculations also predict that the arylation of benzoquinone **4** should proceed at a faster rate than that of the protonated pyridine **1**, in contradiction to the experimental results shown in Figure 1. However, a competition experiment carried out with both substrates **1** and **4** present in the reaction flask helped to shed light on the intrinsic rate difference between the two reactions. Figure 9 compares the temporal product formation of **3** and **5** from parallel reactions carried out in separate flasks with the same products formed in reactions where **1** and **4** are present in the same flask. While the rate of benzoquinone **4** arylation is hardly altered by the presence of pyridine **1** in the flask, the arylation rate of **1** is suppressed by nearly 6-fold in the presence of **4**.

The role of mass transfer across phase boundaries may again be invoked to help reconcile these disparate results. The intrinsic rate of the arylation step may be described by eqs 1 and 2:

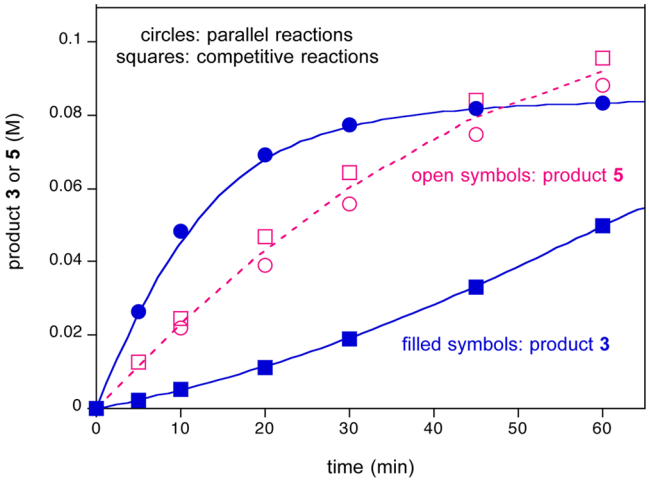

Figure 9. Comparison of temporal product concentration in the arylation of **1** to form **3** (filled blue symbols) and arylation of **4** to form **5** (open pink symbols) carried out in parallel flasks (circles, reproduced from Figure 1) or in competition in the same flask (squares). Conditions: 0.1 M **1** or **4**; 0.15 M **2**; 20 mol % $Ag(NO_3)$, 0.3 M $(NH_4)_2S_2O_8$; CH_2Cl_2:H_2O = 1:1; T = 25 °C. Reactions with **1** include 1 equiv of TFA (see Supporting Information).

$$r(\mathbf{3}) = k_1 \cdot [\mathbf{1}]_{aq} \cdot [Ar^{\bullet}]_{aq}^{eq} \quad (1)$$

$$r(\mathbf{5}) = k_4 \cdot [\mathbf{4}]_{aq} \cdot [Ar^{\bullet}]_{aq}^{ss} \quad (2)$$

The calculated transition states address k_1 and k_4, but these values are not extracted simply from the observed reaction rates, which also depend on substrate concentrations. For reaction of **1**, the concentration term $[\mathbf{1}]_{aq}$ simply equals the total concentration of **1** since it resides in the aqueous phase. For **4** and **2**, however, the aqueous phase concentrations will not equal the total concentrations of **4** and **2**, since a large fraction of these substrates exists in the organic phase. A further complication in comparing experimental rates for reactions in

DOI: 10.1021/acscentsci.5b00332
ACS Cent. Sci. 2015, 1, 456−462

parallel flasks arises because the concentration [Ar•] in the aqueous phase may not be the same during reaction of **1** as it is during reaction of **4**. The reaction of **1** may proceed under a quasi-equilibrated aqueous phase concentration of **2**, and therefore $[Ar^{\bullet}]_{aq}$ is given the superscript "eq" in eq 1. The much faster intrinsic kinetics predicted for **4** may deplete the $[Ar^{\bullet}]_{aq}$ from its equilibrium concentration to give a lower steady-state concentration (given the superscript "ss" in eq 2). During competitive reactions in the same flask, by contrast, the concentration of Ar• will necessarily be the same for reactions of both **1** and **4**, and under these conditions substrate **1** will necessarily encounter the lower steady-state concentration of Ar•, since the reaction of **4** is proceeding simultaneously. Therefore, the 6-fold decrease in rate of production of **3** in the competitive reaction compared to the separate flask reaction may be attributed to a 6-fold lower concentration of Ar• available under these conditions.

We can further combine the experimental and computational results to estimate the true concentration of **4** in the aqueous phase as follows. The relative rates of the two reactions under competitive conditions is given by eq 3, where the steady-state concentration of Ar• is the same for both substrates and therefore cancels. The difference in transition state $\Delta G^{\ddagger}$ obtained from Figure 8 (**TSa-1** 10.7 kcal/mol versus **TSa-4** 8.1 kcal/mol) equates to a predicted rate constant ratio that is 81-fold higher for k_4 over k_1. With $[\mathbf{1}]_0$ = 0.1 M and the observed 6-fold rate difference in initial rates observed in Figure 9, the concentration of **4** in the aqueous phase is estimated using eq 4 to be ca. 7% of its total concentration of 0.1 M.

$$\left(\frac{r_{[3]}}{r_{[5]}}\right)_{\text{competitive}} = \frac{k_1}{k_4}\cdot\frac{[\mathbf{1}]_{aq}}{[\mathbf{4}]_{aq}}\cdot\frac{[Ar^{\bullet}]^{ss}_{aq}}{[Ar^{\bullet}]^{ss}_{aq}} \tag{3}$$

$$\frac{1}{6} = \frac{1}{81}\cdot\frac{0.1\ \text{M}}{[\mathbf{4}]_{aq}} \tag{4}$$

Thus, the intrinsic kinetics of the reaction between **4** and **2** is masked by the presence of mass transfer processes that mediate the concentration of both **2** and **4** between phases. For the reaction of **1**, the intrinsic kinetic dependence on [**1**] is observed as it undergoes rate-determining addition of Ar• in the aqueous phase.

The interplay between chemical and physical processes for these reaction steps is illustrated in Scheme 2. Formation of Ar• occurs in the aqueous phase after diffusion of **2** across the phase boundary. Ar• reacts in a rate-determining step with either **1** or **4**, with the large difference in their aqueous phase concentrations acting to diminish the intrinsic reactivity difference between the two substrates. C–H abstraction step occurs after the rate-determining addition of Ar•, as confirmed by the lack of a deuterium kinetic isotope effect. The product of each reaction is observed in the organic phase at the end of the reaction, requiring a further diffusion step across the phase boundary for both **3** and **5** as well as deprotonation for **3**. Scheme 2 reconciles all of the results from the global kinetic studies, the KIE results, the mass spectroscopic results, and the computational modeling.

While these phase transfer rate processes add complexity to the chemical kinetics of the reaction, they also provide a parameter for reaction optimization. Mediation by the aqueous/organic phase boundary ensures that a steady supply of aryl radicals is available on demand for the intrinsic kinetic

Scheme 2. Reaction and Mass Transfer Steps in the Two-Phase Reactions of Scheme 1

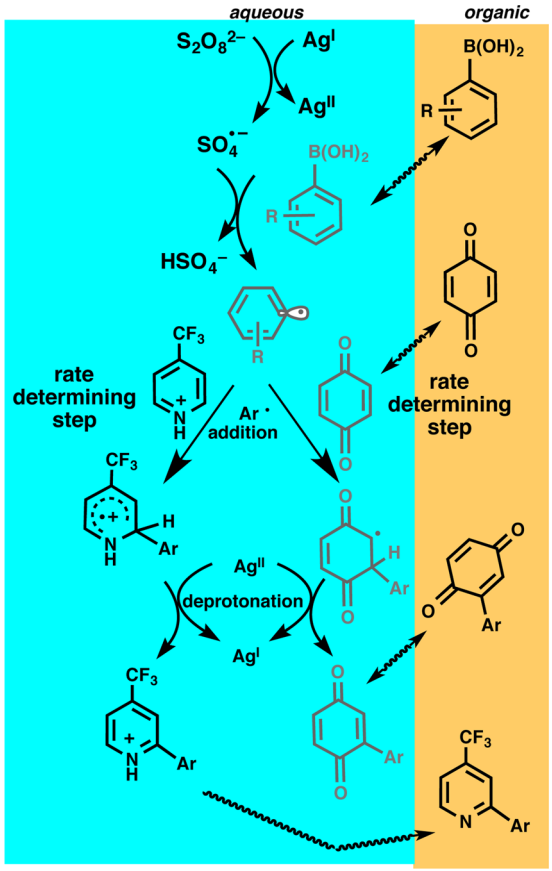

steps of the reaction in the aqueous phase either with substrate **1**, which resides primarily in this phase, or with substrate **4**, which diffuses into the aqueous phase. Limiting the concentration of **2** in the vicinity of the persulfate may also help reaction yield by inhibiting unproductive pathways that are accessed when free radical concentration in the vicinity of reactants is too high. Indeed, attempts to carry out these reactions under homogeneous conditions—either in the aqueous phase by using water-soluble trifluoroborate salts or in the organic phase by using acid-free conditions for the pyridine substrates—led to dramatically lower yields (see Supporting Information). The use of other solvent mixtures that can solubilize all components also led to unacceptably low yields. Under two-phase conditions, mass transfer rate processes that judiciously mediate concentrations for chemical reaction steps can become an important optimization tool.

Kinetic and spectroscopic studies link the observation of anomalous zero-order kinetics in arylboronic acid concentration to phase transfer considerations, both in producing free radicals from the oxidant and in utilizing these free radicals in the reaction. Comparison of global reaction rate profiles with the relative rates and selectivities of competitive reactions reveals that intrinsic chemical kinetics may be convoluted with rates of mass transfer across phase boundaries. The Ag^{I}–Ag^{II} redox mechanism originally proposed for this catalytic cycle appears to apply generally to both pyridine and benzoquinone substrates without the need to invoke the formation of organometallic catalysts. This work may be generally useful for unlocking mechanistic details of multiphase reactions and, in particular, deciphering and deconvoluting chemical and mass

DOI: 10.1021/acscentsci.5b00332
ACS Cent. Sci. 2015, 1, 456–462

transport kinetic processes. It may also encourage the development of bi- or multiphasic reaction conditions for other transformations where mass transfer rate processes can help mediate intermediate concentrations in individual chemical reaction steps.

■ ASSOCIATED CONTENT

Supporting Information

The Supporting Information is available free of charge on the ACS Publications website at DOI: 10.1021/acscentsci.5b00332.

Procedures, data, results, and computational details (PDF)

■ AUTHOR INFORMATION

Corresponding Authors

*E-mail: blackmond@scripps.edu.
*E-mail: pbaran@scripps.edu.
*E-mail: houk@chem.ucla.edu.
*E-mail: rnz@stanford.edu.

Notes

The authors declare no competing financial interest.

■ ACKNOWLEDGMENTS

D.G.B. and P.S.B. acknowledge funding from NIH/NIGMS (GM-106210) and Pfizer, Inc. D.G.B., K.N.H., and R.N.Z. acknowledge funding from the NSF Centers for Chemical Innovation: Center for Catalytic C−H Functionalization (CCHF, CHE-1205646). R.D.B. acknowledges NIH-NIGMS Ruth L. Kirschstein postdoctoral fellowship. Helpful discussions with Prof. Dennis P. Curran are gratefully acknowledged. We acknowledge D.-H. Huang and L. Paternack (TSRI NMR Facility) for valuable assistance with NMR spectroscopy.

■ REFERENCES

(1) Sun, Y.-K.; Landau, R. N.; Wang, J.; LeBlond, C.; Blackmond, D. G. *J. Am. Chem. Soc.* **1996**, *118*, 1348−1353.

(2) Schotten, C. *Ber. Dtsch. Chem. Ges.* **1884**, *17*, 2544. Baumann, E. *Ber. Dtsch. Chem. Ges.* **1886**, *19*, 3218.

(3) Rideout, D. C.; Breslow, R. *J. Am. Chem. Soc.* **1980**, *102*, 7816−7817.

(4) Narayan, S.; Muldoon, J.; Finn, M. G.; Fokin, V. V.; Kolb, H. C.; Sharpless, K. B. *Angew. Chem., Int. Ed.* **2005**, *44*, 3275−3279.

(5) Sebastian Cabeza, V.; Kuhn, S.; Kulkarni, A. A.; Jensen, K. F. *Langmuir* **2012**, *28*, 7007−7013.

(6) Mansy, S. S.; Schrum, J. P.; Krishnamurthy, M.; Tobe, S.; Treco, D. A.; Szostak, J. W. *Nature* **2008**, *454*, 122−125.

(7) Lackner, A. D.; Samant, A. V.; Toste, F. D. *J. Am. Chem. Soc.* **2013**, *135*, 14090−14093.

(8) (a) Seiple, I. B.; Su, S.; Rodriguez, R. A.; Gianatassio, R.; Fujiwara, Y.; Sobel, A. L.; Baran, P. S. *J. Am. Chem. Soc.* **2010**, *132*, 13194−13196. (b) Fujiwara, Y.; Domingo, V.; Seiple, I. B.; Gianatassio, R.; Del Bel, M.; Baran, P. S. *J. Am. Chem. Soc.* **2011**, *133*, 3292−3295.

(9) For selected reviews on the Minisci reaction, see: (a) Minisci, F.; Vismara, E.; Fontana, F. *Heterocycles* **1989**, *28*, 489. (b) Minisci, F.; Fontana, F.; Vismara, E. J. *J. Heterocycl. Chem.* **1990**, *27*, 79. (c) Harrowven, D. C.; Sutton, B. J. *Prog. Heterocycl. Chem.* **2005**, *16*, 27−53.

(10) For recent examples of radical arylations based on the described methods, see: (a) Fang, L.; Shi, X.; Chen, L.; Yu, J.; Wang, L. *Synlett* **2014**, *25*, 1413−1418. (b) Bonin, H.; Sauthier, M.; Felpin, F.-X. *Adv. Synth. Catal.* **2014**, *356*, 645−671. (c) Komeyama, K.; Nagao, Y.; Abe, M.; Takaki, K. *Bull. Chem. Soc. Jpn.* **2014**, *87*, 301−313. (d) Komeyama, K.; Kashihara, T.; Takaki, K. *Tetrahedron Lett.* **2013**, *54*, 1084−1086. (e) Singh, P. P.; Aithagani, S. K.; Yadav, M.; Singh, V. P.; Vishwakarma, R. A. *J. Org. Chem.* **2013**, *78*, 2639−2648. (f) Guan, D.; Huang, Y. *J. Chem. Res.* **2013**, *37*, 649−651. (g) Deb, A.; Manna, S.; Maji, A.; Dutta, U.; Maiti, D. *Eur. J. Org. Chem.* **2013**, *2013*, 5251−5256. (h) Mahindra, A.; Jain, R. *Synlett* **2012**, *23*, 1759−1764. (i) Lamblin, M.; Naturale, G.; Dessolin, J.; Felpin, F.-X. *Synlett* **2012**, *23*, 1621−1624. (j) Wang, J.; Wang, S.; Wang, G.; Zhang, J.; Yu, X.-Q. *Chem. Commun.* **2012**, *48*, 11769−11771.

(11) Patel, N. R.; Flowers, R. A. *J. Am. Chem. Soc.* **2013**, *135*, 4672−4674; *J. Am. Chem. Soc.* **2013**, *135*, 7788.

(12) We have been unable to reproduce the negative order dependence on arylboronic acid **2** concentration reported in the mechanistic study of the reaction with **1** reported in ref 11, and we suggest that mass transfer issues may have caused an anomalous result in that study. Partitioning of substrates and products between phases can lead to erroneous concentrations unless the entire reaction vial contents are included upon workup. Monitoring both decay of substrate and appearance of product can use the mass balance to determine whether concentrations are accurately represented after reaction workup. In the reactions employed to determine the order in [arylboronic acid] in ref 11, only the decay of [**1**] was monitored to determine order in [**2**], although in some other reactions in that study both substrate decay and product growth were reported.

(13) Ingram, A. J.; Solis-Ibarra, D.; Zare, R. N.; Waymouth, R. M. *Angew. Chem., Int. Ed.* **2014**, *53*, 5648.

(14) Fürmeier, S.; Metzger, J. O. *J. Am. Chem. Soc.* **2004**, *126*, 14485.

(15) Paiva, A. A.; Tilton, R. F., Jr.; Crooks, G. P.; Huang, L. Q.; Anderson, K. S. *Biochemistry* **1997**, *36*, 15472−15476.

(16) Sabino, A. A.; Machado, A. H. L.; Correia, C. R. D.; Eberlin, M. N. *Angew. Chem., Int. Ed.* **2004**, *43*, 2514.

(17) Santos, L. S. *Eur. J. Org. Chem.* **2008**, *2008*, 235.

(18) Simmons, E. M.; Hartwig, J. F. *Angew. Chem., Int. Ed.* **2012**, *51*, 3066.

(19) We make the assumption that the H/D composition of the molecules does not significantly influence the mass transfer rate across phase boundaries.

DOI: 10.1021/acscentsci.5b00332
ACS Cent. Sci. 2015, 1, 456−462